Impact of temporal resolution of precipitation forcing data on modelled urban-atmosphere exchanges and surface conditions

INTERNATIONAL JOURNAL OF CLIMATOLOGY
Int. J. Climatol. (2017)
Published online in Wiley Online Library
(wileyonlinelibrary.com) DOI: 10.1002/joc.5200

RMetS
Royal Meteorological Society

Impact of temporal resolution of precipitation forcing data on modelled urban-atmosphere exchanges and surface conditions

H. C. Ward,[a,*] Y. S. Tan,[a,b] A. M. Gabey,[a] S. Kotthaus[a] and C. S. B Grimmond[a]
[a] *Department of Meteorology, University of Reading, Reading, UK*
[b] *Labaun Meteorological Office, Malaysian Meteorological Department, Labaun, Malaysia*

ABSTRACT: Representative precipitation data sets are very difficult to obtain due to the inherent spatial and temporal variability of rainfall. Gridded rainfall products exist at various scales, but temporal resolution is coarse (daily or, at best, a few hours). This study demonstrates the impact of low temporal resolution precipitation forcing data (PFD) on modelled energy fluxes, runoff and surface conditions, which could have implications for a range of applications including flood forecasting, irrigation scheduling and epidemiology. An evaporation-interception model originally developed for forests is applied here within the framework of the Surface Urban Energy and Water balance Scheme (SUEWS). The model is forced with rainfall data representative of a range of temporal resolutions (from 5 min to 3 h). Taking the highest resolution case as a reference, differences in model output are found as the temporal resolution of PFD decreases, depending on the timing of rainfall occurrence, intensity and duration. Modelled evaporation, runoff and surface wetness deviate from the reference case, which affect other variables such as the turbulent sensible heat flux. The largest impacts are seen on days with greatest daily total rainfall and, even on days with no rain, differences in antecedent conditions (soil moisture or surface wetness) can cause deviations from the reference case. Errors can be reduced by applying a disaggregation scheme that provides a more realistic distribution of rainfall, importantly, one that allows for intermittent rainfall.

KEY WORDS cities; energy balance; evaporation; rainfall; runoff; water balance

Received 10 February 2017; Revised 6 June 2017; Accepted 10 June 2017

1. Introduction

Given the changing climate and predicted increase in frequency and severity of extreme weather (e.g. Meehl and Tebaldi, 2004; Lehtonen *et al.*, 2014), knowledge of the earth-atmosphere system is becoming more and more important. The ability of weather and climate models to accurately predict or forecast depends on (1) how successfully physical processes are represented by model parameterisations and (2) the quality or suitability of the input data. This study focuses on the latter, specifically the sensitivity of the model to the temporal resolution of precipitation forcing data (PFD).

Precipitation supplies moisture to the surface and is either intercepted and stored in the canopy, infiltrates into the soil, becomes runoff, or is evaporated. It therefore plays an important role in both the water balance and the energy balance, as moisture availability affects the partitioning of energy between the turbulent sensible heat flux and turbulent latent heat flux (evaporation). Evaporation can occur via transpiration from plants, from the soil surface, from open water, or from surfaces that are wet. High-evaporation rates from wet surfaces directly following precipitation events can be substantial (Wouters *et al.*, 2015). For example, Ramamurthy and Bou-Zeid (2014) showed that following precipitation events over a wet 10-day period, nearly 17% of the total latent heat flux was from impervious surfaces. Evidence of increased evaporation rates 12–18 h after rain has been observed in central London (Kotthaus and Grimmond, 2014) and in Toulouse (Wouters *et al.*, 2015).

The transformation of natural surfaces into urban surfaces significantly modifies the local hydrological cycle. In the urban canopy, evaporation is often reduced relative to natural soil and vegetation surfaces. The abundance of impervious surfaces (such as buildings, streets and parking lots) increases surface runoff rates, reduces infiltration and hence increases the total runoff water volumes (e.g. Xiao *et al.*, 2007). These surfaces also restrict water storage capacity (Oke, 1982) but can support high-evaporation rates for a short time following rainfall (Wouters *et al.*, 2015). Providing sufficient moisture is available, the fraction of vegetation cover has also been shown to be a major factor determining the partitioning of energy over urban areas (e.g. Grimmond and Oke, 2002; Christen and Vogt, 2004). Accurate modelling of the urban environment is important both for the resident population, and to simulate the impact that urban areas have on the surrounding weather and climate (Shepherd, 2005; Zhong and Yang, 2015).

The spatial and temporal variability of precipitation can present a significant source of uncertainty in weather and

* Correspondence to: H. C. Ward, Department of Meteorology, University of Reading, Earley Gate, Reading RG6 6BB, UK. E-mail: h.c.ward@reading.ac.uk

climate models (Fekete *et al.*, 2004; Aronica *et al.*, 2005; Wang *et al.*, 2009). According to Berne *et al.* (2004), rainfall data at a temporal resolution of a few minutes is required for hydrological applications in urban areas. However, for practical and financial reasons, there is a discrepancy between what would be optimal for model input and the data that are available from observations (Berne *et al.*, 2004; Licznar *et al.*, 2011). *In situ* measurements require a high density of rain gauges to capture the spatial variability, particularly for rain showers associated with local convection. As for all observations, data quality can be compromised by inappropriate siting, instrument errors or maintenance issues. Sampling errors associated with tipping bucket data at short timescales (Habib *et al.*, 2001) present an additional obstacle to obtaining accurate fine-scale data. Radar networks offer high temporal resolution and good spatial coverage for monitoring the development and evolution of rain events [e.g. 5 min and 1 km in the UK (Golding, 1998)], but are less useful in terms of quantitative accuracy (Kitchen and Illingworth, 2011). Based on historical rain gauge observations, the CEH-GEAR (Centre for Ecology and Hydrology Gridded Estimates of Areal Rainfall) product has a spatial resolution of 1 km for the UK but is only available at a temporal resolution down to 1 day (Keller *et al.*, 2015). Historical reanalysis data (Weedon *et al.*, 2011; Weedon *et al.*, 2014) or future climate predictions may only be available at coarse temporal resolution (e.g. 3 h, 6 h or daily).

To address the discrepancy between observations (or climate model output) and required model input, numerous disaggregation schemes have been developed (Gaume *et al.*, 2007; Willems and Vrac, 2011; Pui *et al.*, 2012). However, many only disaggregate down to the daily time scale (Maraun *et al.*, 2010), whereas much higher temporal resolution is required for urban areas (Grimmond and Oke, 1991) or small, steep catchments (Cowpertwait *et al.*, 2007). In the very simplest downscaling approach, an even distribution of rainfall (i.e. constant intensity) is assumed, whereby equal amounts of rainfall are distributed across every subinterval. A slightly more advanced approach is the cascade model (Sivakumar and Sharma, 2008), where rainfall at the coarsest resolution is unevenly distributed among smaller and smaller subintervals until the desired resolution is reached. One issue with this approach is that all subintervals of a disaggregated rainy period contain at least some rain (i.e. there are no dry periods). Using precipitation data collected in Australia, Sivakumar and Sharma (2008) obtain no dry periods in their disaggregated data set but demonstrate using their observed rainfall time series that dry periods occur about 30% of the time. This problem with cascade models not predicting zero values is also highlighted in Gaume *et al.* (2007). It is not the intention here to explore in detail the various rainfall disaggregation schemes; for reviews, the reader is referred to Srikanthan and McMahon (2001) or Maraun *et al.* (2010). Rather, here we aim to demonstrate the impact of limited temporal resolution of PFD on the modelled urban water balance, energy fluxes and surface state.

Hydrometeorological models are being increasingly used in hazard-warning and decision-making capacities, that is, the outcome of models is used to influence decisions taken by citizens, government or advisory bodies. Understanding the uncertainties and limitations associated with model output is therefore of prime importance. Incorrect calculation of the water balance has obvious implications for flood forecasting (when, where and how significant will flooding be?) and drainage design (what is a suitable capacity for a storm sewer?), but can also be problematic for irrigation planning and greenspace management. Knowledge of whether the urban surface is wet or dry is relevant for epidemiology (e.g. spread of water-borne diseases, or risk of mould developing) as well as road safety, particularly in near-freezing conditions. Accurate simulation of the surface energy balance is important for predicting urban heat island intensity and thermal comfort. Sensible heat flux plays a key role in determining boundary-layer development, which has implications for air quality. Hence errors in the input forcing data, particularly those affecting moisture availability, can have far-reaching consequences.

Other studies investigating the effects of temporal resolution of PFD on rainfall-runoff models include the impact on urban drainage systems in Italy (Aronica *et al.*, 2005) and on urban discharge in France (Berne *et al.*, 2004). However, studies investigating the impact on the water balance, surface energy balance and surface conditions are limited. The focus of this study is on how these modelled quantities are affected by the resolution of PFD, what are the implications of the bias introduced by using low resolution PFD and how can this bias be minimized. The analysis uses data from a suburban case-study site (Swindon) in the south of the UK, but sensitivity analyses and the physical explanation for the findings suggest the results are widely applicable.

2. Methodology

2.1. The model

An evaporation-interception model originally developed for forests (Gash, 1979) and later adapted for urban areas (Grimmond and Oke, 1991) is applied here. The physical basis of the model is a running water balance for each surface (Grimmond *et al.*, 1986):

$$P + I_e + F = E + R + \Delta S \tag{1}$$

where, P is precipitation, E is evaporation (including transpiration), R is runoff, and ΔS is the net change in water storage (e.g. soil moisture, water stored in the canopy). In urban areas, additional inputs including I_e the external piped water supply and F anthropogenic water emissions (e.g. from combustion, air conditioning, human respiration) can be supplied if appropriate; these are neglected here. Evaporation is calculated using the Penman–Monteith approach (Monteith, 1965) using surface resistances. The model is run within the framework of the Surface Urban Energy and Water balance Scheme

(SUEWS), which also simulates the energy fluxes (Oke, 1987):

$$Q^* + Q_F = Q_H + Q_E + \Delta Q_S \quad (2)$$

where, Q^* is net all-wave radiation, Q_F is anthropogenic heat flux, Q_H is turbulent sensible heat flux, Q_E is turbulent latent heat flux ($Q_E = L_v E$; L_v is latent heat of vaporization), and ΔQ_S is net storage heat flux.

The water balance calculations (Järvi *et al.*, 2011) are performed as follows. For each surface (except water), j, drainage, D, is calculated as a function of the amount of water on the canopy, C, using (Halldin *et al.*, 1979):

$$D_j = D_0 \exp\left(bC_j - 1\right) \quad (3)$$

for vegetated surfaces, with the coefficients $D_0 = 0.013\,\text{mm h}^{-1}$ and $b = 171\,\text{mm}^{-1}$ (Grimmond and Oke, 1991), and (Falk and Niemczynowicz, 1978):

$$D_j = D_0 C_j^b \quad (4)$$

for non-vegetated surfaces, with the coefficients $D_0 = 10\,\text{mm h}^{-1}$ and $b = 3$ (Grimmond and Oke, 1991). Naturally, no drainage occurs if the canopy is dry. Drainage can occur between surface types according to a redistribution matrix set in the input files. For Swindon, water from pervious surfaces infiltrates into the soil stores beneath; 2% of water from paved surfaces flows to grass, 2% of water from roofs flows to grass and 8% of water flows from roofs to paved surfaces with the remaining proportions becoming runoff into pipes. These proportions are judged based on knowledge of the study area and are identical to those used for the model evaluation. No water can infiltrate directly into the soil stores beneath paved or building surfaces (Järvi *et al.*, 2011).

Evaporation is calculated using the Penman–Monteith approach (Monteith, 1965) using surface resistance, r_s, based on a Jarvis–Stewart formulation (Jarvis, 1976; Grimmond and Oke, 1991; Järvi *et al.*, 2011; Ward *et al.*, 2016); r_s for dry conditions (i.e. without surface moisture storage) is calculated first, then adjusted according to the surface wetness state (Shuttleworth, 1978). When the surface is completely wet r_s is set to zero. This threshold above which each surface is assumed to be completely wet, C_{wet}, must be set in the input information; the values used (Table 1) were initially set using the storage capacities as an estimate based on values from the literature (Falk and Niemczynowicz, 1978; Davies and Hollis, 1981; Breuer *et al.*, 2003), then adjusted slightly based on comparison with observations in Swindon and London (Ward *et al.*, 2016). When the surface is partially wet, the adjusted r_s that is used in the Penman–Monteith equation is given by (Shuttleworth, 1978),

$$r_{s\,adj} = \left[\frac{W}{r_b\left(\frac{s}{\gamma}+1\right)} + \frac{(1-W)}{r_s + r_b\left(\frac{s}{\gamma}+1\right)}\right]^{-1} - r_b\left(\frac{s}{\gamma}+1\right) \quad (5)$$

where, r_b is the boundary layer resistance, s the slope of the saturation vapour pressure curve, γ the psychrometric constant and W is a function of the surface wetness state. If C_{wet} is exceeded, W is set to 1 and $r_{s\,adj} = 0$ (completely wet surfaces). If $C < C_{wet}$,

$$W = \frac{K-1}{K - \frac{C_{wet\,i}}{C_i}} \quad (6)$$

with

$$K = \frac{r_s\left(r_a - r_b\right)}{r_a\left(r_s + r_b\left(\frac{s}{\gamma}+1\right)\right)} \quad (7)$$

where, r_a is the aerodynamic resistance for water vapour.

Water can evaporate from the canopy of wet surfaces and from the single-layer soil store below pervious surfaces; if impervious surfaces are dry the evaporation from pervious surfaces is increased correspondingly, representing oasis-type advection in suburban environments (Oke, 1979; Grimmond *et al.*, 1986; Spronken-Smith *et al.*, 2000). No water can evaporate directly from the soil store beneath impervious surfaces (i.e. the model neglects cracks in pavements or partially permeable construction materials). The running water balance (Equation (1)) yields the change in water storage for each surface. If precipitation intensity exceeds a maximum infiltration of $10\,\text{mm h}^{-1}$ (Grimmond and Oke, 1986), the excess becomes runoff. Finally, horizontal transfer of soil water occurs according to the Green and Ampt equation (Hillel, 1971) with soil conductivities according to van Genuchten (1980). Further details and equations are given in Järvi *et al.* (2011).

SUEWS has been evaluated using observations from North American cities (Järvi *et al.*, 2011); Helsinki (Järvi *et al.*, 2014; Karsisto *et al.*, 2015); Montreal (Järvi *et al.*, 2014); Dublin (Alexander *et al.*, 2015; Alexander *et al.*, 2016); Hamburg, Melbourne and Phoenix (Alexander *et al.*, 2016); Singapore (Demuzere *et al.*, 2017); and two UK sites: suburban Swindon and central London (Ward *et al.*, 2016). In this study, SUEWS v2017a (Ward *et al.*, 2017) is run offline for a single grid point representative of the Swindon site (Section 2.2). The model time-step is 5 min and output is provided at resolutions of 5 min and 60 min.

Required inputs are basic meteorological data (incoming shortwave radiation $K_\downarrow$, air temperature, relative humidity, atmospheric pressure, wind speed and precipitation), surface characteristics and information about energy and water use within the study area. The model typically requires 60-min meteorological forcing data which are first processed to 5-min resolution. This is done using linear interpolation (except for rainfall), which is generally reasonable as most of these variables change smoothly throughout the day.

In the absence of more detailed information about the fine-scale distribution of precipitation, the simplest assumption is to assume rainfall is evenly distributed. This has the potential to affect the water balance, and

Table 1. Summary of model inputs (Ward *et al.*, 2016).

Surface type	Paved	Buildings	Evergreen	Deciduous	Grass	Bare soil	Water
Surface cover fraction	0.33	0.16	0.01	0.08	0.36	0.06	0.00
Albedo	0.10	0.12	0.10	0.12–0.18	0.18–0.21	0.18	0.10
Threshold for wet evaporation (mm)	0.60	0.60	1.80	1.00	2.00	1.00	0.50
Moisture storage capacity (mm)	0.48	0.25	1.30	0.30–0.80	1.90	0.80	0.50
Soil storage capacity (mm)	150	150	150	150	150	150	-
Study area							
Population density (ha^{-1})	47.63						
Mean building/tree height (m)	4.5[a]/6.2						
Roughness length (m)	0.5						
Displacement height (m)	3.5						

The range of albedo and moisture storage capacity values represents the seasonal minimum and maximum. [a]note mean building height is incorrectly given as 4.2 m in Ward *et al.* (2016).

hence energy partitioning. To investigate the impact of this assumption, multiple model runs are performed differing only by the temporal resolution of the PFD provided. The downscaled meteorological variables are combined with eight different 5-min time series of precipitation data. The observed 5-min precipitation time series is used as a reference. Each of the remaining precipitation data time series are created by summing the 5-min data to various averaging periods (10, 15, 30, 60, 90, 120 and 180 min) and then downscaling back to 5-min assuming an even distribution of rainfall within each averaging period. Model output from the 5-min reference case therefore represents the 'best-case', and any deviations from this reference case indicate errors caused by using lower temporal resolution PFD. This approach eliminates the need to compare model output against observed data, which would introduce a range of other uncertainties. Indeed, this approach allows the effect of temporal resolution of PFD to be isolated from other sources of variation between model and observations.

For completeness, observations are shown alongside modelled output in (Figure 1) and Appendix. At the Swindon site SUEWS simulates the turbulent sensible and latent heat fluxes well [$r^2 = 0.79$ and 0.72, respectively, based on 2 years of 60-min data (Ward *et al.*, 2016)]. For the period analysed here (2012) evaporation is slightly underestimated compared to observations (Figure 1b). Given the potential discrepancies between observed and modelled data sets (e.g. due to variable measurement footprint, uncertainties in the observations) the agreement is remarkable. Wetting and drying trends are captured well in the soil moisture data (Figure 1a), especially during summer and considering that the modelled data represent the whole study area whilst the observed data are from a single probe beneath grass. Seasonal variation in the energy fluxes is modelled well (Ward *et al.*, 2016) and at shorter timescales, the model is capable of capturing hourly changes in the turbulent fluxes, soil moisture and surface wetness state in response to rainfall (Appendix). Successful simulation of surface wetness state compared to observations was also obtained in Vancouver (Grimmond and Oke, 1991). No runoff observations were available for Swindon, however, previous evaluation in Helsinki showed good agreement with measured data (Järvi *et al.*, 2014).

2.2. Study area and observations

The required meteorological forcing data were measured at a suburban site in Swindon, UK (51°35′N, 1°48′W, 108 m above sea level). The high-resolution (5-min) rainfall data were measured with a tipping bucket rain gauge (0.2 mm tip, Casella CEL, Bedford, UK) and gap-filled from nearby sites. Surface characteristics required to run SUEWS (Table 1) are identical to the model evaluation (Ward *et al.*, 2016) and are representative of the area surrounding the measurement site. Soil stores were initially set to 80% of their saturation value. Irrigation was assumed to be negligible given the wet climate (Alexander *et al.*, 2015). The 'open low-rise' local climate zone (Stewart and Oke, 2012) characterizes the area well. The area is very typical of UK suburban residential areas. Further details about the site and instrumentation are given in Ward *et al.* (2013).

During the study period (1 January to 31 December 2012) there were 223 days with rain and 136 days with observed rainfall >1.0 mm (Figure 2). The annual rainfall for 2012 was 1020.2 mm. The climate normal (1981–2010) for southern England is 793.9 mm (Met Office, 2016). Overall, 2012 was wetter than normal, with the wettest months being April, June and December with 127.8, 133.8 and 135.0 mm rain, respectively. However, the first 3 months of 2012 were drier than normal. The maximum daily rainfall intensity of 29.4 mm day^{-1} occurred on 29 April 2012. The longest period without appreciable (>1.0 mm) daily rainfall lasted 23 days from 31 August to 22 September. The longest period without any observed rain lasted 14 days, from 20 March to 2 April 2012.

3. Results

3.1. Impact of temporal resolution on rainfall data

Altering the temporal resolution of precipitation forcing data has two important effects: as the averaging period increases (or temporal resolution decreases) the peak

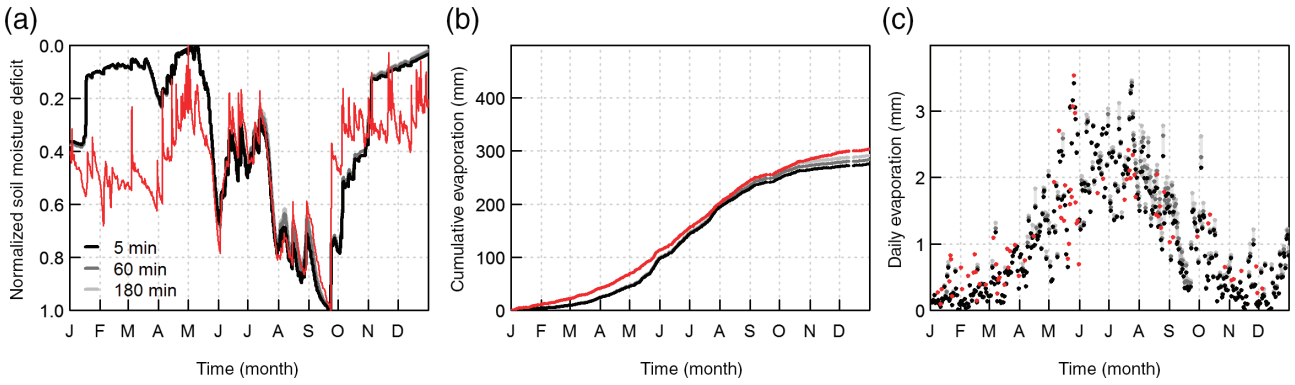

Figure 1. Modelled (using 5-, 60- and 180-min precipitation forcing data) and observed (red) (a) normalized soil moisture deficit, (b) cumulative evaporation and (c) daily evaporation for Swindon in 2012. Observed and modelled cumulative totals in (b) contain only those times when observations are available. In (c) observed data are shown only for days with 100% data coverage.

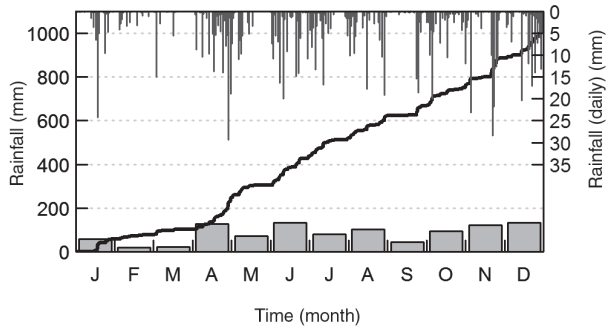

Figure 2. Observed precipitation for Swindon in 2012: daily, monthly and cumulative totals.

intensities are lost and the number of 5-min periods with non-zero rainfall increases (Figure 3). For example, an original 5-min time series with periods of no rain, light rain and heavy rain (Figure 3a) is transformed into light rain of longer duration (Figure 3h). In this example, the maximum rainfall intensity was 0.80 mm in 5 min at 20:05 (Figure 3a) but at 180-min resolution this is decreased to 0.15 mm for every 5-min period between 18:05 and 21:00 (Figure 3h). While the original 5-min time series has 20 periods of rainfall (52 without), there are no dry periods for resolutions coarser than 120 min (Figure 3f-h). Note the total rainfall over the 6-h period is unchanged. Figure 4 shows the relative proportions of wet and dry 5-min periods over the whole year. The 5-min data set indicates rainfall occurs 4% of the time but assuming an even distribution of rainfall based on 60-min or 180-min forcing data would result in rainfall 13 or 22% of the time.

3.2. Impact on the energy and water balance

These differences in the intermittency and intensity of rainfall impact the energy and water balance, illustrated in Figure 5 for an example day. Column A is the reference case, for which the 5-min precipitation data indicates intermittent rain with maximum recorded intensity of 0.6 mm in 5 min. The prolonged duration of rainfall at lower temporal resolutions means the surface tends to stay wet for longer (row 1–2 of Figure 5). Evaporation rates are higher when surfaces are wet, particularly in urban environments where moisture availability is often limited by the abundance of impervious materials with limited storage capacity. High evaporation rates from wet surfaces are clearly seen in the evolution of the latent heat flux (row 3), particularly at 5-min resolution when the sharp peaks in surface wetness state are matched by peaks in Q_E. The reduction in rainfall intensity also causes a reduction in runoff: the peak runoff for the reference case is 0.41 mm in 5 min; when using 60-/180-min PFD peak runoff decreases to is 0.13 mm/0.06 mm in 5 min (row 1). Hence at lower temporal resolutions, not only is total runoff underestimated compared to the 5-min reference case (row 4 of Figure 5) but also peak runoff rates are also missed. Although the differences in daily totals are quite small, importantly, the error accumulates over time because runoff is more frequently underestimated (rather than overestimated) when using low temporal resolution PFD.

As the temporal resolution of PFD decreases the modelled soil moisture deficit is also increasingly underestimated compared to the 5-min reference case (i.e. soils are slightly moister when lower temporal resolution PFD are used, Figure 1a). The reduction in rainfall intensity and modelled runoff, and prolonged duration of wet surfaces, increases infiltration leading to an overestimation in soil moisture (although the effect is much smaller than for runoff or evaporation). These slightly increased reserves of soil moisture also contribute to the overestimation of evaporation.

In this study, the model parameterisations used are such that Q^*, Q_F and ΔQ_S are not affected by the temporal resolution of PFD. Therefore, the available energy for partitioning into turbulent heat fluxes is independent of the temporal resolution of PFD. This is a limitation of the model; studies have shown that wet surfaces can modify Q^* (both through the outgoing longwave radiation and albedo) and ΔQ_S (Kawai and Kanda, 2010; Frey *et al.*, 2011; Wouters *et al.*, 2015; Sun *et al.*, 2017). As SUEWS calculates Q_H as the residual of the energy balance (Equation (2)), an overestimation of Q_E will result in an underestimation of Q_H compared to the reference case. It follows that the

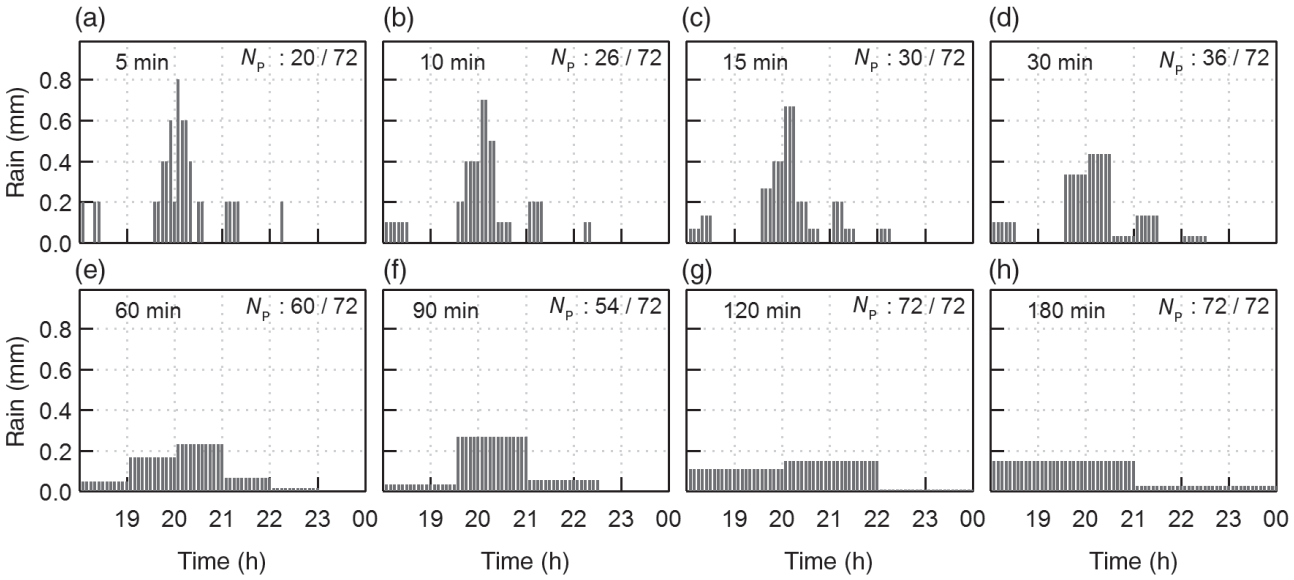

Figure 3. Example rain events (Swindon, 04 April 2012) redistributed over different temporal resolutions. Each bar indicates the 5-min rainfall value. The number of 5-min periods with rain >0 mm (N_P) is shown in each panel.

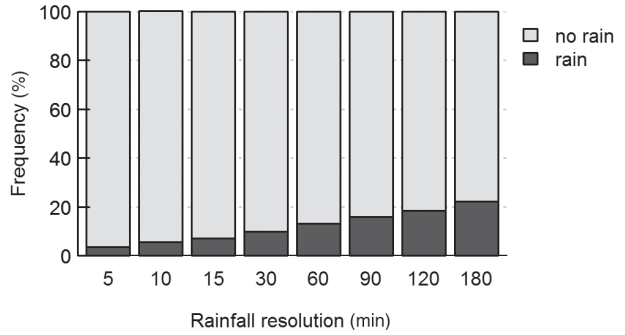

Figure 4. Relative frequency of 5-min periods with rain (>0 mm) for 2012 in Swindon for different temporal resolutions of precipitation forcing data assuming rainfall is evenly distributed.

Bowen ratio ($\beta = Q_H/Q_E$) will also be underestimated compared to the reference case. For the example in Figure 5, mean daytime β decreases from 0.42 to 0.28 to 0.16 going from 5-min to 60-min to 180-min resolution. For this suburban site, a small proportion of Q_H is supported by the anthropogenic heat flux ($\approx$5–10 W m^{-2}). For more densely built-up sites with larger Q_F the relative impact of temporal resolution on Q_H would be smaller (because Q_F largely supports Q_H), but the increased proportion of impervious surface cover means the relative impact on Q_E would be larger (because total Q_E would be smaller) (Section 3.3.1).

Overall, as the temporal resolution of PFD decreases modelled evaporation is increasingly overestimated and modelled runoff is increasingly underestimated compared to the reference case. To investigate this behaviour more closely the total daily evaporation, E_i, for each resolution, i, is normalized by the total daily evaporation for the reference case, E_5 (Figure 6a). Days with more rainfall tend to experience a larger overestimation in evaporation. When the daily total rainfall amount is small, the impact on the daily evaporation is smaller and daily total evaporation may be higher ($E_i/E_5 > 1$) or lower ($E_i/E_5 < 1$) than the reference case. For days with no rain (grey lines in Figure 6a), temporal resolution of PFD generally has a small effect. As the forcing data is identical for these days (no rain in any 5-min period, irrespective of the resolution), the differences in evaporation are a result of the differences in antecedent conditions, namely surface and soil moisture states, caused by the change in intensity and duration of rainfall on previous days with rain.

There are 116 days in the data set with no runoff ($R_5 = 0$ mm); these have been excluded from the normalized daily runoff analysis (Figure 6b). The runoff ratio shows more variability than the evaporation ratio, particularly for days with low total precipitation when the reference runoff, R_5, is small (the $P = 0$ mm line in Figure 6b is therefore not important). Considering the absolute difference between daily runoff for each resolution and the reference case ($R_i - R_5$), larger changes are observed for wetter days, as is also the case for evaporation. However, wetter days generate more runoff so, for the same absolute difference, normalization by R_5 will result in a smaller percentage difference for wetter days. In terms of the annual water budget, the reference case gives a total evaporation of 374.7 mm. Using PFD at a resolution of 60-min (180-min) increases the total by 13.4 mm (24.7 mm), which is 3.6% (6.6%) larger than the reference case. For runoff, the reference case is 624.4 mm, which decreases by 14.1 mm at 60-min resolution and 25.4 mm at 180-min resolution.

3.3. Sensitivity studies

3.3.1. Surface cover

Surface cover is one of the main controls on the partitioning of energy and water fluxes. The availability of sub-surface moisture and the drainage behaviour varies between surface types. The impact of temporal resolution

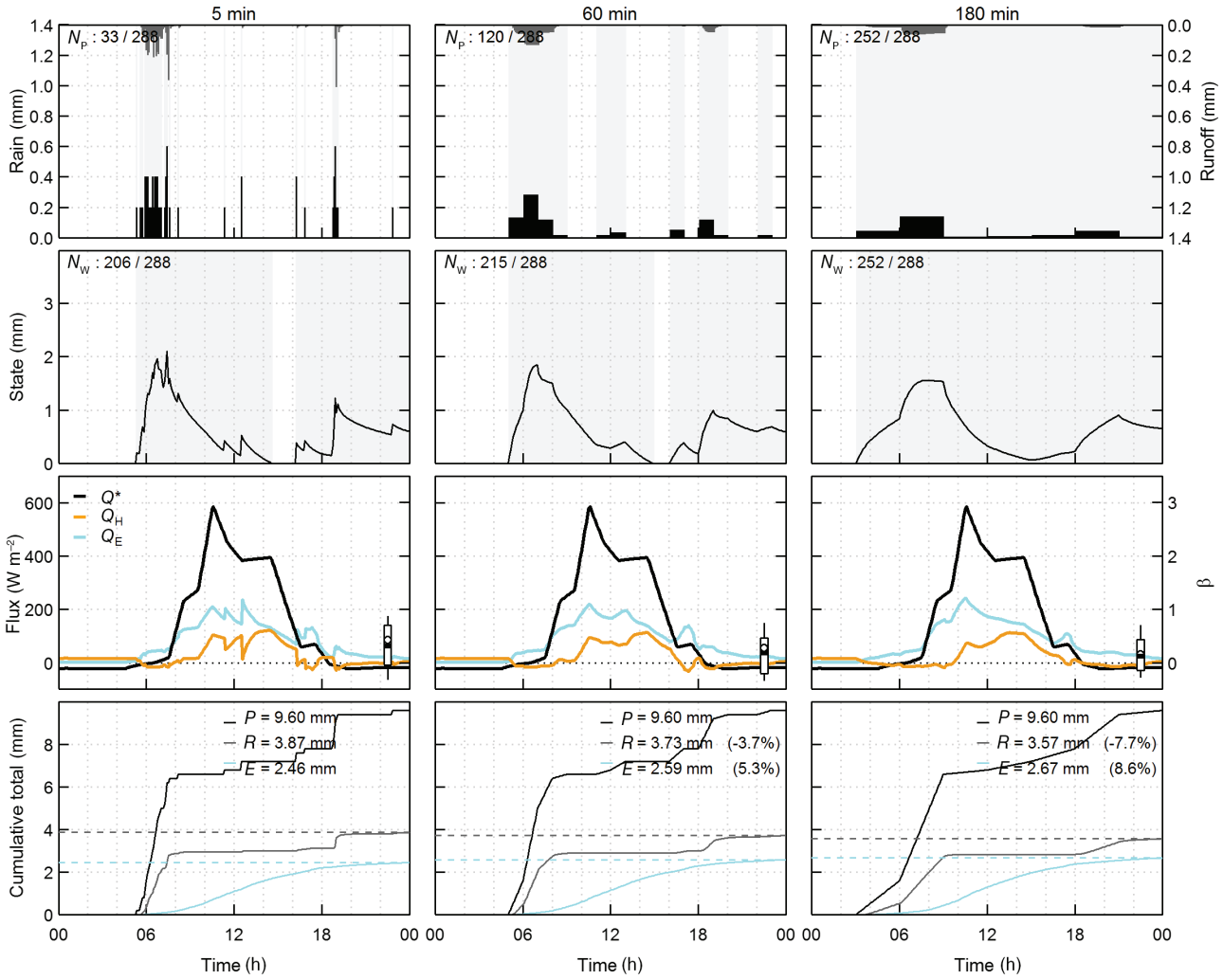

Figure 5. Rainfall distribution, surface wetness state, energy fluxes (net all-wave radiation Q^*, sensible heat flux Q_H, latent heat flux Q_E) and cumulative water balance for 5 August 2012 in Swindon using precipitation forcing data at a temporal resolution of 5, 60 and 180 min (each data point plotted represents 5 min). The number of 5-min periods with rain (N_P) and when the surface is wet (N_W) are given (and also indicated by shading). The daily total precipitation (P), runoff (R) and evaporation (E) are given in row 4, along with the percentage change in runoff and evaporation compared to the reference case. The boxplots in row 3 show the distribution of daytime Bowen ratio (when incoming shortwave radiation $K_\downarrow > 5$ W m^{-2}). Boxes indicate the median and inter-quartile range, whiskers the 10th and 90th percentiles and open circles the mean value.

of PFD will presumably be greater for regions with a larger proportion of impervious surfaces, as these surfaces have very low evaporation under dry conditions but can support very high evaporation rates when wet (Ramamurthy and Bou-Zeid, 2014; Ward *et al.*, 2015). This is supported by Figure 7, which shows the annual difference in modelled evaporation and runoff for different resolutions of PFD for a range of surface cover fractions. The setup is the same as for the model runs presented above, but here the surface cover fractions have been modified. The results for 10% buildings, 10% deciduous trees, 40% grass and 40% paved surfaces are very similar to the results for the Swindon site, as the surface cover proportions are similar (Table 1). As the proportion of paved surface is increased at the expense of grass, the absolute difference between E_i and E_5 decreases (Figure 7a). However, because the total evaporation is also reduced for areas with more paved surfaces/less vegetation, the relative overestimation in evaporation increases (Figure 7b). For runoff, the impact of temporal resolution of PFD is largest (in both relative and absolute terms) for more vegetated surfaces. Reducing the intensity and increasing the duration of rainfall increases infiltration into soils beneath vegetated surfaces, decreasing runoff. For impervious surfaces, as almost all water becomes runoff, total runoff is less sensitive to rainfall intensity and duration.

3.3.2. *Model parameters*

To investigate the sensitivity of these results to model parameters, further model runs were performed (Table 2). SUEWS specifies a maximum infiltration rate of 10 mm h^{-1}, above which rainfall is assumed to go straight to runoff. Precipitation is rarely expected to exceed the maximum infiltration rate (Grimmond and Oke, 1986), and does so for <0.1% of the data here. Therefore, increasing the maximum infiltration rate makes little difference to the results, as there are already very few occurrences

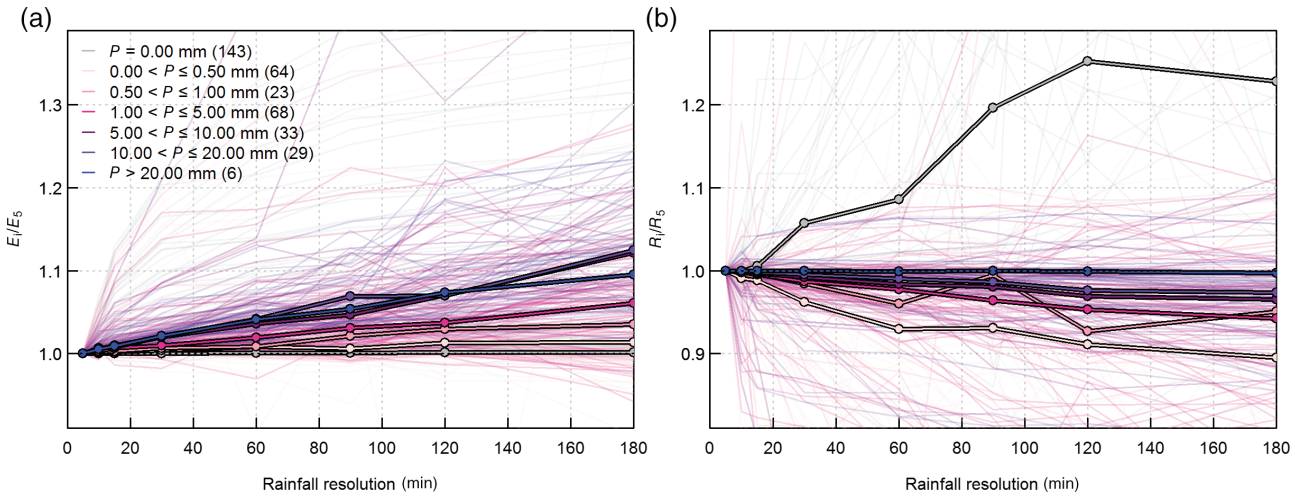

Figure 6. Daily total (a) evaporation E and (b) runoff R normalized by the reference case (subscript 5) for various temporal resolutions of precipitation forcing data (subscript i) for Swindon 2012. Each line represents an individual day coloured according to daily total rainfall P (legend, number of days given in brackets). Thick lines indicate median values. In (b) days with $R_5 = 0$ mm have been excluded to avoid division by zero. If the rainfall resolution had no impact on the evaporation (runoff) rate then E_i/E_5 (R_i/R_5) would be 1.

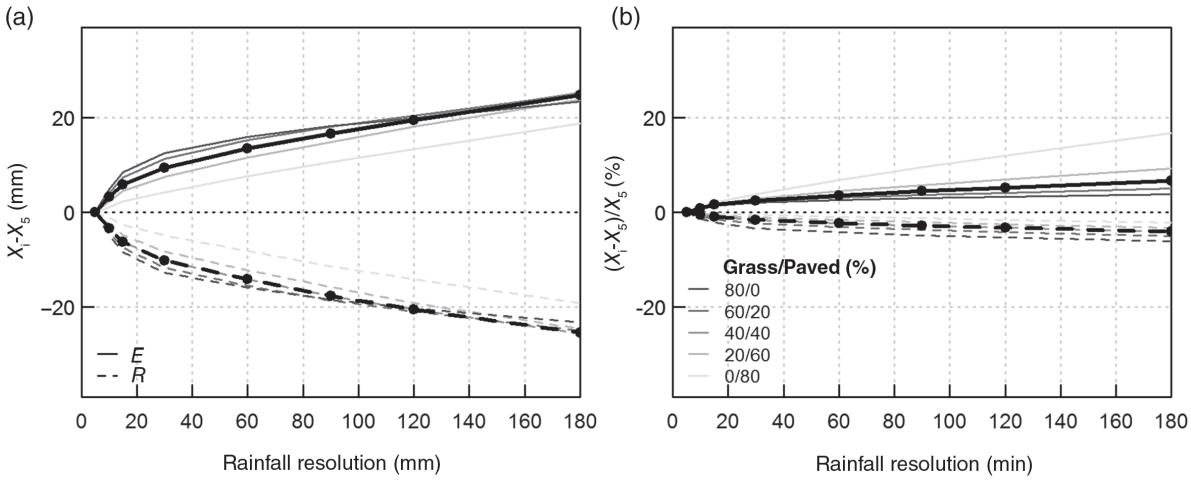

Figure 7. Annual (a) absolute difference and (b) percentage difference in water balance components (X_i) from the 5-min reference case (X_5) for the Swindon study site (filled circles) and for different surface cover fractions (10% buildings, 10% deciduous trees and percentage grass/paved surfaces as given in the legend) for 2012. E denotes evaporation, R denotes runoff.

of this threshold being exceeded. Lowering the maximum infiltration rate to 5 mm h^{-1} makes more of a difference, as a greater proportion of the dataset exceed the lower threshold. In this case, more water is directed to runoff and less to evaporation. The impact of temporal resolution of PFD is greater because the threshold is exceeded more often in the reference case, but still not very often with 180-min PFD.

Other parameters affecting the distribution of water in the model include the wetness threshold above which evaporation is assumed to occur from totally wet surfaces [i.e. surface resistance is set to zero (Järvi *et al.*, 2011; Ward *et al.*, 2016)]. For the current model setup, surface storage capacities are not used in the drainage equations (Equations (3) and (4)) and therefore do not impact the results. Soil storage capacities have a small effect on the results (Table 2), with temporal resolution of PFD having a slightly larger impact for greater soil storage capacities. Increasing the threshold for wet evaporation slightly reduces the impact of temporal resolution. Increasing this threshold reduces the frequency with which evaporation occurs assuming totally wet surfaces, decreasing evaporation under wet or partially wet conditions so surfaces remain wet for longer. The prolonged surface wetness associated with temporal resolution of PFD therefore makes less of an impact.

Initialisation of soil moisture can have a significant effect on model output (Best and Grimmond, 2014). However, the temporal resolution of PFD affects the data in the same way for different initial values (60, 80 and 100% of saturation were tested, Table 2). For initially wetter soils the impact is slightly reduced, for initially drier soils the impact is increased, presumably because more of the total annual evaporation comes from wet surfaces when soils are drier and the frequency of surfaces being wet is greater with lower resolution PFD.

Table 2. Results of the sensitivity analysis for various model parameters for Swindon in 2012.

Model run	E_5 (mm)	$E_{180}-E_5$ (mm)	$(E_{180}-E_5)/E_5$ (%)	R_5 (mm)	$R_{180}-R_5$ (mm)	$(R_{180}-R_5)/R_5$ (%)
Base run	374.7	24.7	6.6	624.4	−25.4	−4.1
Infiltration rate 5 mm h^{-1}	361.7	37.0	10.2	639.0	−39.2	−6.1
Infiltration rate 15 mm h^{-1}	378.6	20.8	5.5	620.1	−21.1	−3.4
Soil storage capacity 120 mm	383.3	23.2	6.1	646.9	−24.2	−3.7
Soil storage capacity 180 mm	369.2	25.6	6.9	607.1	−25.6	−4.2
Threshold for wet evaporation −20%	382.5	27.1	7.1	616.9	−27.8	−4.5
Threshold for wet evaporation +20%	367.9	22.9	6.2	631.0	−23.6	−3.7
Initial soil moisture 60%	370.3	25.4	6.9	605.8	−25.5	−4.2
Initial soil moisture 100%	378.4	24.1	6.4	648.7	−25.0	−3.9

The base run parameters are as specified in Table 1 and a maximum in infiltration rate of 10 mm h^{-1}.

This analysis demonstrates that although the magnitude of the impact of temporal resolution of PFD varies slightly depending on the model parameters, the overall results do not change.

3.3.3. Other meteorological forcing variables

Of the other meteorological forcing variables, the temporal resolution of incoming shortwave radiation is thought to have the next most significant impact after rainfall (Kokkonen *et al.*, 2017; Ward and Grimmond, 2017), partly because large changes in $K_{\downarrow}$ can occur over time scales of a few minutes. However, the impact of temporal resolution of $K_{\downarrow}$ on the water balance is found to be much smaller than for precipitation. Compared to the 5-min reference case (5-min rainfall, 5-min $K_{\downarrow}$), annual evaporation modelled using 60-min (180 min) $K_{\downarrow}$ is 1.8 mm (4.1 mm) larger, corresponding to a percentage increase of 0.5% (1.1%). For runoff, the difference is even smaller (−3.6 mm or −0.6% at 180 min).

The largest changes in $K_{\downarrow}$ often occur during summer daytimes with patchy cloud cover, however, the impact of the $K_{\downarrow}$ fluctuations usually average out and the longer-term variation (∼hourly timescales) in $K_{\downarrow}$ is generally captured by the mean values. For the example day shown in Figure 5, $K_{\downarrow}$ forcing data were provided at a resolution of 60-min and have been linearly interpolated to 5-min. Repeating the runs with 5-min PFD and 5-, 60- and 180-min resolution $K_{\downarrow}$ produces smaller deviations from the reference dataset: differences of <1% at 60-min and −1.5% (runoff) and 3.0% (evaporation) at 180-min. For other days, the difference is in the opposite direction (i.e. overestimated runoff and underestimated evaporation). As linearly downscaled $K_{\downarrow}$ deviates from the reference case *in both directions* there is far less of a bias compared to downscaling precipitation using methods which lead to non-zero rainfall in every subinterval.

3.4. Recommendations

In this section, simple approaches to downscaling precipitation forcing data are considered. In the absence of more detailed information about the fine-scale distribution of precipitation, the simplest assumption is that rainfall is evenly distributed across all 5-min subintervals within each averaging period (i.e. constant intensity). This method is referred to as 'uniform' disaggregation and has been shown to be unrealistic (Section 3.1–3.3). An alternative approach, where rainfall is unevenly distributed across all 5-min subintervals ('non-uniform') improves matters slightly (Figure 8, Table 3). However, substantial improvements are achieved by distributing rainfall across fewer subintervals and allowing some subintervals to be without rain. When PFD is evenly distributed over half the subintervals ('0.50 N' case), the over/underestimation in evaporation/runoff compared to the 5-min reference case is reduced further. The annual total modelled evaporation underestimates the observations (Figure 1), so the augmented evaporation as a result of coarse temporal resolution of PFD actually brings modelled values closer to observations. However, there are numerous reasons for differences between modelled and observed evaporation (e.g. imperfect parameterisation, slightly inappropriate parameter values, variable source area characteristics, measurement uncertainties). Therefore, comparison to the 5-min reference case is more appropriate for this study focusing solely on the impact of temporal resolution of PFD. When PFD is evenly distributed over one quarter of the subintervals ('0.25 N'), the over/underestimation in evaporation/runoff is substantially reduced at 180 min, while at 60 min the direction of the bias is reversed: evaporation is now underestimated and runoff overestimated compared to the reference case.

Analysis of the 5-min reference dataset used here suggests that only about 0.3% of 60-min periods have rainfall in all 12 constituent 5-min subintervals, and there are zero 180-min periods with rainfall recorded in all 36 constituent 5-min subintervals. The average number of rainy 5-min subintervals in each 60-min period is 3.34 of 12; for 180-min it is 5.96 of 36. Using this information the PFD was disaggregated by evenly distributing rainfall across the mean number of rainy subintervals (rounded to the nearest whole number of subintervals). For example, the total rainfall in each 60-min period was distributed evenly between three randomly selected 5-min subintervals within the 60-min period whilst the remaining nine subintervals were assigned zero rainfall. This method is denoted 'meanN'. This approach substantially reduces the bias for 180-min, but performs similarly to the 0.25 N approach at 60-min. This is not surprising, as in both cases 60-min rainfall is distributed among 3 of 12

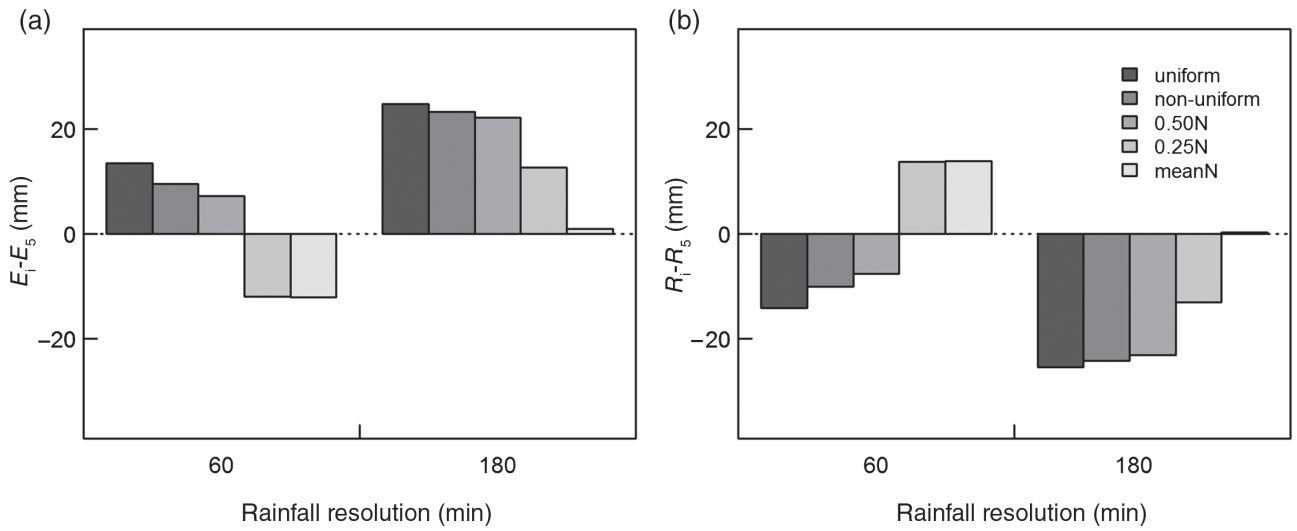

Figure 8. Annual difference in (a) evaporation E and (b) runoff R for 60-and 180-min precipitation forcing data (subscript i) downscaled to 5-min (subscript 5) using various disaggregation methods (legend) for Swindon 2012.

Table 3. Results of the disaggregation schemes. $N_{P\,180}$ is the number of 5-min subintervals with rainfall following disaggregation of 180-min precipitation forcing data according to the different disaggregation methods.

Downscaling method	$N_{P\,180}$ (%)	$E_{180} - E_5$ (mm)	$(E_{180} - E_5)/E_5$ (%)	$R_{180} - R_5$ (mm)	$(R_{180} - R_5)/R_5$ (%)
uniform	22.3	24.7	6.6	−25.4	−4.1
non-uniform	22.3	23.2	6.2	−24.2	−3.9
0.50 N	11.2	22.1	5.9	−23.0	−3.7
0.25 N	5.6	12.7	3.4	−13.0	−2.1
meanN	3.7	0.9	0.3	0.3	<0.1

Total annual evaporation E_5 is 374.7 mm and runoff R_5 is 624.4 mm for the reference case (Table 2). The number of 5-min periods with rainfall for the reference case is 3.7%. The results for 'uniform' downscaling are the same as those for the base run (Table 2).

subintervals. Since the mean number of rainy subintervals in 60-min is actually 3.34, distributing rainfall across only 3 subintervals causes an overestimation in intensity and underestimation in the number of rainy periods, which explains why the meanN and 0.25 N methods change the sign of the bias. For 180-min PFD, the 0.25 N approach distributes rainfall across 9 subintervals, which is greater than the mean value of 5.96, hence the 0.25 N approach still over/underestimates evaporation/runoff at 180-min. Since 5.96 is close to 6.00, the meanN approach performs well for this 180-min data set. Note that due to the random sampling involved in these disaggregation methods, the exact values obtained for repeat runs vary slightly (differences of <1 mm in annual totals) but the overall findings remain unchanged (i.e. the performance of the disaggregation methods remains similar, even if the modelled values change slightly).

3.5. Discussion of limitations

Meteorological conditions during the study period combine to influence evaporation and runoff totals, and the type of rain event affects the impact of using lower temporal resolution PFD (Figure 6). In the UK, stratiform precipitation is very common and rain generally falls as low-intensity showers rather than high-intensity storms (it is, however, important to correctly represent high-intensity storms, even if they occur only rarely, due to the severity of their potential impacts on population and infrastructure). If this study were repeated for a site with a more concentrated rainfall distribution it is expected that temporal resolution would have an even larger impact. Although 2012 contained both very wet periods and very dry periods, results may vary for other years. However, the overall findings are expected to be similar. No clear differences with season were identified for this dataset, which is not surprising given the UK climate. In other locations, it may be appropriate to apply a different disaggregation for different types of rainfall (e.g. convective storms during summer; monsoon seasons). For example, initial analyses show the average number of rainy subintervals in Shanghai varies with season and precipitation intensity (W. Gu, 2017; personal communication).

The number of rainy subintervals within each period is negatively skewed. The mean value alone cannot capture all relevant information about the distribution about rainfall occurrence or rainfall intensity, however, these results show that the number of rainy/non-rainy subintervals is a key parameter when downscaling; whether rainfall is evenly or unevenly distributed has a smaller effect (Figure 8). It is also important that realistic intensities are preserved in the disaggregated data set, particularly for the highest intensities, as water that cannot infiltrate will become runoff. The occurrence and distribution of rainfall

will also vary with location, season and type of rainfall, as well as the observational technique. For example, a 5-min radar time-series for a nearby site has a higher frequency of rainy subintervals than observed by the tipping bucket, but the overall impact of the temporal resolution of PFD was very similar. These are all factors which complicate the disaggregation of rainfall, and local calibration may be required for more complex schemes. If detailed information or complex disaggregation schemes are unavailable, distributing rainfall to allow some subintervals without rain is more appropriate than evenly distributing rainfall to all subintervals (Section 3.4).

To isolate the impact of temporal resolution of PFD, this study aims to remove many uncertainties (such as the representativeness of input data, specification of initial values and characterization of the surface) by comparing results to the 5-min reference case. Therefore, the analysis considers only those changes that result from a change in temporal resolution of the precipitation forcing data. However, models are always only an approximation of reality and not all processes and interdependencies may be represented. For example, surface albedos in SUEWS are specified for each surface type but currently do not change with surface wetness state. Evaporation of rainfall has also been shown to affect outgoing longwave radiation; a reduction of about 10 W m^{-2} was found in Toulouse (Wouters *et al.*, 2015). Similarly, the dependence of storage heat flux on moisture conditions (Kawai and Kanda, 2010; Wouters *et al.*, 2015) was not accounted for in this study, but could be explored in future using a more sophisticated parameterisation for storage heat flux (e.g. Sun *et al.*, 2017). Lastly, the selection of input parameters to accurately represent the modelled area of interest remains a challenge for modellers and users of models. This should be a focus for future observational campaigns in urban areas. In this study, the size of the difference between observations and model is similar to, but larger than, the differences due to temporal resolution of PFD (Figure 1), reflecting these other limitations and uncertainties of model-observation comparisons. However, accurate provision of input data is fundamental to model development; if a model was to perform perfectly with inaccurate input data, the model physics or parameterisations must somehow compensate for these inaccuracies.

4. Conclusions

The impact of the temporal resolution of precipitation forcing data on modelled surface energy and water balance is investigated. Results demonstrate that as the temporal resolution decreases, rainfall intensity is reduced and rainfall duration is prolonged, leading to reduced runoff rates and lower runoff in total, increased infiltration resulting in moister soils, surfaces remaining wet for longer, and increased evaporation. The size of the impact increases as the temporal resolution decreases. Compared to the 5-min resolution case taken as a reference, annual evaporation may be overestimated and annual runoff underestimated by some tens of mm (or 5–10%) for resolutions of 60–180 min. Changes in daily evaporation and runoff totals show considerable variation, as the impact of temporal resolution depends on many factors including the intensity and duration of the rain event, energy availability and antecedent conditions. Days with appreciable rainfall generally have higher evaporation totals and lower runoff for coarser temporal resolution PFD; days with little or no rainfall are less affected by the resolution of PFD but can have lower evaporation totals and higher runoff due to differences in antecedent conditions (e.g. soil moisture differences or an altered rain distribution on the previous day causing surfaces to remain wet for longer and supporting runoff). At low temporal resolution, not only is total runoff underestimated but peak runoff rates are also missed. Although these results are based on the SUEWS framework, the physical explanation for the deviations from the reference case suggest similar effects are likely with other models based on the same principles. This hypothesis could be tested in future. Since evaporation appears in the energy balance as the latent heat flux term, PFD also affect the energy partitioning. Overestimated latent heat flux results in an underestimated sensible heat flux and, therefore, an underestimated Bowen ratio, with implications for boundary-layer development and air quality.

This study demonstrates that using 60-min observations or 180-min reanalysis (or climate prediction) data as forcing data assuming rainfall to be evenly distributed will result in errors in modelled output of the order of 5–10%. Although the temporal resolution of incoming shortwave radiation forcing data has a small impact on the model output, generally these short-term fluctuations about the mean average out so linearly downscaling $K_{\downarrow}$ introduces far less of a bias than for precipitation. To improve accuracy, either PFD of finer spatial and temporal resolution is needed (which presents practical and financial challenges) or more advanced schemes for disaggregating rainfall data should be used. Only the temporal aspect has been considered here, but making a very simple adjustment to the disaggregation scheme so that rainfall is not distributed to every 5-min subinterval within each averaging interval showed a reduction in the overestimation of evaporation and underestimation of runoff resulting from low temporal resolutions. For this study the 5-min data were available to inform this improved disaggregation procedure. However, further investigation of rainfall patterns at other sites and over different years is warranted. This would help to improve the accuracy of rainfall disaggregation where high resolution data are not available and thus to reduce model bias. It is expected that temporal resolution would have an even larger impact at sites with a more concentrated distribution of rainfall or during specific storm hazards. Better representation of precipitation forcing data should improve model performance and avoid both the short-term impacts of missing peak runoff rates (important for flood prediction and town planning) and the long-term effects of model bias with implications for annual totals and interpretation with respect to climate change.

The SUEWS model is available to download from http://micromet.reading.ac.uk.

Acknowledgements

We would like to thank everyone who assisted with the data collection. We thank the World Meteorological Organization and the Malaysian Meteorological Department for supporting Yin San Tan's MSc studies. Additionally, this work was funded by the following projects: NERC/Belmont TRUC NE/L008971/1, G8MUREFU3FP-2201-075; UK-China Research & Innovation Partnership Fund through the Met Office Climate Science for Service Partnership (CSSP) China as part of the Newton Fund. Wen Gu's visit from Shanghai Institute of Meteorological Sciences was funded by CSSP-China.

Appendix: SUEWS model output compared to observations

Observed and modelled turbulent heat fluxes, soil moisture and surface wetness state are shown for 11 (example)

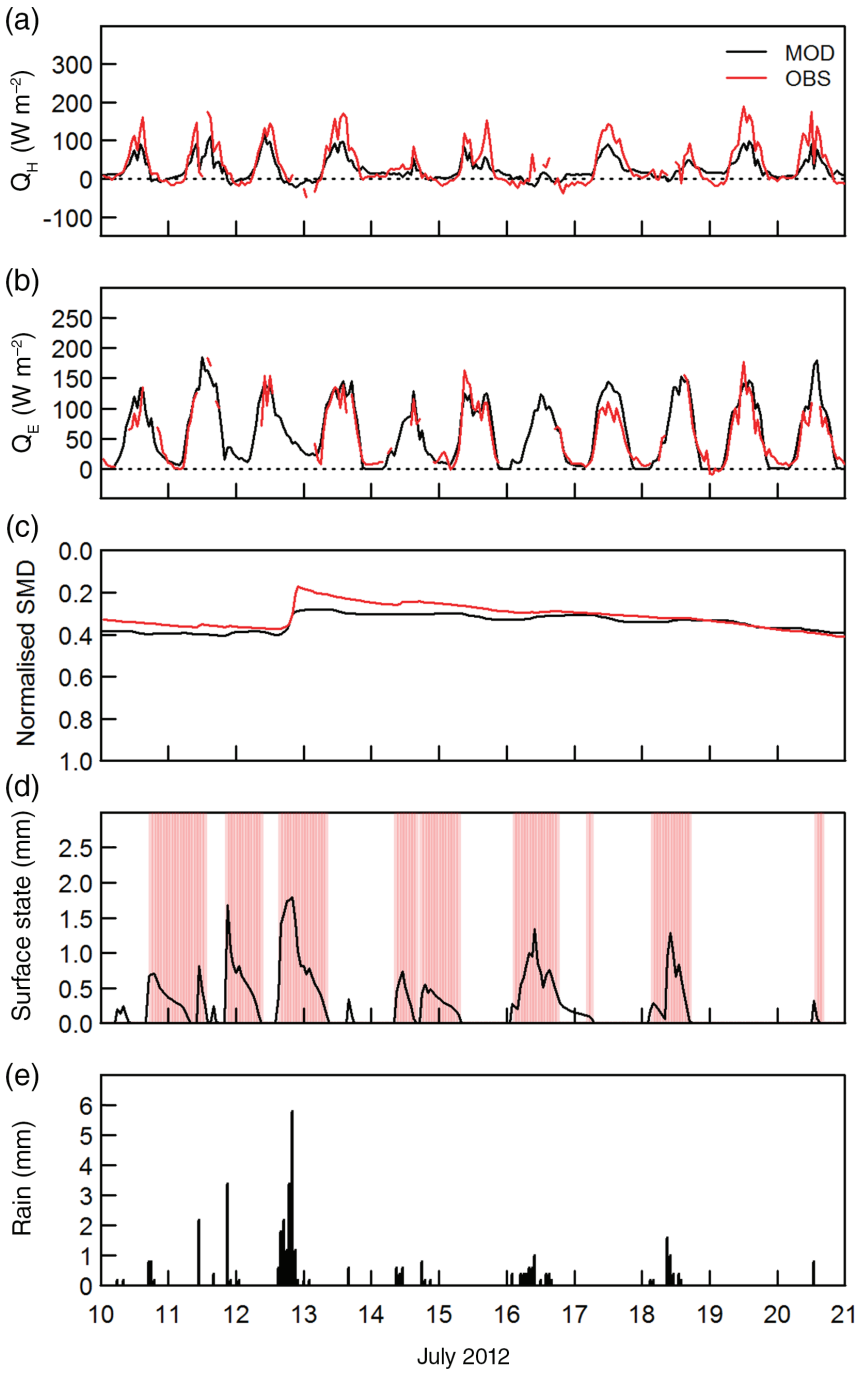

Figure A1. Modelled and observed (a) sensible heat flux, Q_H, (b) latent heat flux, Q_E, (c) normalized soil moisture deficit (SMD) and (d) surface wetness state (shading indicates observed wet periods), and (e) observed rainfall for Swindon for 10–20 July 2012.

days in July 2012 (Figure A1). Observed turbulent heat fluxes were obtained from a sonic anemometer (R3, Gill Instruments) and infrared gas analyser (LI-7500, LI-COR Biosciences) installed at 12.5 m on a mast in the garden of a residential property in suburban Swindon. Observed soil moisture was measured (CS616, Campbell Scientific Ltd.) at a depth of 0.03–0.05 m beneath grass lawn in the garden. In Figure A1, observed and modelled soil moisture deficits have been normalized by their respective maximum and minimum values for 2012. Observed surface wetness is provided by a wetness sensor (model 237, Campbell Scientific Ltd.) installed near the base of the mast, which indicates wet/dry conditions but does not provide water volumes. As the soil moisture probe and wetness sensor are point measurements they are not expected to represent the study area, but provide a rough indication of the conditions at the site. Further details about the measurements can be found in Ward *et al.* (2013).

References

Alexander PJ, Mills G, Fealy R. 2015. Using LCZ data to run an urban energy balance model. *Urban Clim.* **13**: 14–37. https://doi.org/10.1016/j.uclim.2015.05.001.

Alexander PJ, Bechtel B, Chow WTL, Fealy R, Mills G. 2016. Linking urban climate classification with an urban energy and water budget model: multi-site and multi-seasonal evaluation. *Urban Clim.* **17**: 196–215. https://doi.org/10.1016/j.uclim.2016.08.003.

Aronica G, Freni G, Oliveri E. 2005. Uncertainty analysis of the influence of rainfall time resolution in the modelling of urban drainage systems. *Hydrol. Processes* **19**: 1055–1071. https://doi.org/10.1002/hyp.5645.

Berne A, Delrieu G, Creutin J-D, Obled C. 2004. Temporal and spatial resolution of rainfall measurements required for urban hydrology. *J. Hydrol.* **299**: 166–179. https://doi.org/10.1016/j.jhydrol.2004.08.002.

Best MJ, Grimmond CSB. 2014. Importance of initial state and atmospheric conditions for urban land surface models' performance. *Urban Clim.* **10**: 387–406. https://doi.org/10.1016/j.uclim.2013.10.006.

Breuer L, Eckhardt K, Frede H-G. 2003. Plant parameter values for models in temperate climates. *Ecol. Model.* **169**: 237–293. https://doi.org/10.1016/S0304-3800(03)00274-6.

Christen A, Vogt R. 2004. Energy and radiation balance of a central European city. *Int. J. Climatol.* **24**: 1395–1421. https://doi.org/10.1002/joc.1074.

Cowpertwait P, Isham V, Onof C. 2007. Point process models of rainfall: developments for fine-scale structure. *Proc. R. Society London Ser. A* **463**: 2569–2587.

Davies H, Hollis T. 1981. *Measurements of Rainfall-Runoff Volume Relationships and Water Balance for Roofs and Roads*. Second International Conference on Urban Storm Drainage: Urbana, IL.

Demuzere M, Harshan S, Järvi L, Roth M, Grimmond CSB, Masson V, Oleson KW, Velasco E, Wouters H. 2017. Impact of urban canopy models and external parameters on the modelled urban energy balance in a tropical city. *Q. J. R. Meteorol. Soc.* **143**: 1581–1596. https://doi.org/10.1002/qj.3028.

Falk J, Niemczynowicz J. 1978. Characteristics of the above ground runoff in sewered catchments. In *Urban Storm Drainage*, Helliwell PR (ed). Pentech: London.

Fekete BM, Vörösmarty CJ, Roads JO, Willmott CJ. 2004. Uncertainties in precipitation and their impacts on runoff estimates. *J. Clim.* **17**: 294–304. https://doi.org/10.1175/1520-0442(2004)0170294:UIPATI2.0.CO;2.

Frey CM, Parlow E, Vogt R, Harhash M, Abdel Wahab MM. 2011. Flux measurements in Cairo. Part 1: in situ measurements and their applicability for comparison with satellite data. *Int. J. Climatol.* **31**: 218–231. https://doi.org/10.1002/joc.2140.

Gash JHC. 1979. An analytical model of rainfall interception by forests. *Q. J. R. Meteorol. Soc.* **105**: 43–55. https://doi.org/10.1002/qj.49710544304.

Gaume E, Mouhous N, Andrieu H. 2007. Rainfall stochastic disaggregation models: Calibration and validation of a multiplicative cascade model. *Adv. Water Resour.* **30**: 1301–1319. https://doi.org/10.1016/j.advwatres.2006.11.007.

van Genuchten MT. 1980. A closed-form equation for predicting the hydraulic conductivity of unsaturated Soils. *Soil Sci. Soc. Am. J.* **44**: 892–898. https://doi.org/10.2136/sssaj1980.03615995004400050002x.

Golding BW. 1998. Nimrod: a system for generating automated very short range forecasts. *Meteorol. Appl.* **5**: 1–16. https://doi.org/10.1017/S1350482798000577.

Grimmond CSB, Oke TR. 1986. Urban water-balance 2. Results from a suburb of Vancouver, British-Columbia. *Water Resour. Res.* **22**: 1404–1412.

Grimmond CSB, Oke TR. 1991. An evapotranspiration-interception model for urban areas. *Water Resour. Res.* **27**: 1739–1755.

Grimmond CSB, Oke TR. 2002. Turbulent heat fluxes in urban areas: observations and a local-scale urban meteorological parameterization scheme (LUMPS). *J. Appl. Meteorol.* **41**: 792–810.

Grimmond CSB, Oke TR, Steyn DG. 1986. Urban water-balance 1. A model for daily totals. *Water Resour. Res.* **22**: 1397–1403.

Habib E, Krajewski WF, Kruger A. 2001. Sampling errors of tipping-bucket rain gauge measurements. *J. Hydrol. Eng.* **6**: 159–166. https://doi.org/10.1061/(ASCE)1084-0699(2001)6:2(159).

Halldin S, Grip H, Perttu K. 1979. Model for energy exchange of a pine forest canopy. In *Comparison of Forest Water and Energy Exchange Models*, Halldin S (ed). International Society of Ecological Modeling: Copenhagen, Denmark.

Hillel D. 1971. *Soil and Water: Physical Principles and Processes*. Academic Press: New York, NY.

Järvi L, Grimmond CSB, Christen A. 2011. The surface urban energy and water balance scheme (SUEWS): evaluation in Los Angeles and Vancouver. *J. Hydrol.* **411**: 219–237.

Järvi L, Grimmond CSB, Taka M, Nordbo A, Setälä H, Strachan IB. 2014. Development of the surface urban energy and water balance scheme (SUEWS) for cold climate cities. *Geosci. Model Dev.* **7**: 1691–1711. https://doi.org/10.5194/gmd-7-1691-2014.

Jarvis PG. 1976. The interpretation of the variations in leaf water potential and Stomatal conductance found in canopies in the field. *Phil. Trans. Royal Soc. Lond. B.* **273**: 593–610. https://doi.org/10.1098/rstb.1976.0035.

Karsisto P, Fortelius C, Demuzere M, Grimmond CSB, Oleson KW, Kouznetsov R, Masson V, Järvi L. 2015. Seasonal surface urban energy balance and wintertime stability simulated using three land-surface models in the high-latitude city Helsinki. *Q. J. R. Meteorol. Soc.* **142**: 401–417. https://doi.org/10.1002/qj.2659.

Kawai T, Kanda M. 2010. Urban energy balance obtained from the comprehensive outdoor scale model experiment. Part I: Basic Features of the Surface Energy Balance. *J. Appl. Meteorol. Climatol.* **49**: 1341–1359. https://doi.org/10.1175/2010jamc1992.1.

Keller VDJ, Tanguy M, Prosdocimi I, Terry JA, Hitt O, Cole SJ, Fry M, Morris DG, Dixon H. 2015. CEH-GEAR: 1 km resolution daily and monthly areal rainfall estimates for the UK for hydrological and other applications. *Earth Syst. Sci. Data* **7**: 143–155. https://doi.org/10.5194/essd-7-143-2015.

Kitchen M, Illingworth A. 2011. From observations to forecasts – part 13: the UK weather radar network – past, present and future. *Weather* **66**: 291–297. https://doi.org/10.1002/wea.861.

Kokkonen T, Grimmond C, Räty O, Ward H, Christen A, Oke T, Kotthaus S, Järvi L. 2017. Sensitivity of Surface Urban Energy and Water Balance Scheme (SUEWS) to Downscaling of Reanalysis Forcing Data. *Urban Clim.* https://doi.org/10.1016/j.uclim.2017.05.001.

Kotthaus S, Grimmond CSB. 2014. Energy exchange in a dense urban environment – part I: temporal variability of long-term observations in central London. *Urban Clim.* **10**: 261–280. https://doi.org/10.1016/j.uclim.2013.10.002.

Lehtonen I, Ruosteenoja K, Jylhä K. 2014. Projected changes in European extreme precipitation indices on the basis of global and regional climate model ensembles. *Int. J. Climatol.* **34**: 1208–1222. https://doi.org/10.1002/joc.3758.

Licznar P, Łomotowski J, Rupp DE. 2011. Random cascade driven rainfall disaggregation for urban hydrology: an evaluation of six models and a new generator. *Atmos. Res.* **99**: 563–578. https://doi.org/10.1016/j.atmosres.2010.12.014.

Maraun D, Wetterhall F, Ireson AM, Chandler RE, Kendon EJ, Widmann M, Brienen S, Rust HW, Sauter T, Themeßl M, Venema VKC, Chun KP, Goodess CM, Jones RG, Onof C, Vrac M, Thiele-Eich I. 2010. Precipitation downscaling under climate change: Recent developments to bridge the gap between dynamical models and the end user. *Rev Geophys* **48**: RG3003. https://doi.org/10.1029/2009RG000314.

Meehl GA, Tebaldi C. 2004. More intense, more frequent, and longer lasting heat waves in the 21st Century. *Science* **305**: 994–997. https://doi.org/10.1126/science.1098704.

Met Office. 2016. Climate Averages (1981–2010). www.metoffice.gov.uk/public/weather/climate (accessed 19 Febraury 2016).

Monteith JL. 1965. Evaporation and environment. *Symp. Soc. Exp. Biol.* **19**: 205–224.

Oke TR. 1979. Advectively-assisted evapotranspiration from irrigated urban vegetation. *Bound.-Layer Meteorol.* **17**: 167–173.

Oke TR. 1982. The energetic basis of the urban heat-island. *Q. J. R. Meteorol. Soc.* **108**: 1–24.

Oke TR. 1987. *Boundary Layer Climates*. Routledge, Taylor and Francis Group: London, UK, 435.

Pui A, Sharma A, Mehrotra R, Sivakumar B, Jeremiah E. 2012. A comparison of alternatives for daily to sub-daily rainfall disaggregation. *J. Hydrol.* **470–471**: 138–157. https://doi.org/10.1016/j.jhydrol.2012.08.041.

Ramamurthy P, Bou-Zeid E. 2014. Contribution of impervious surfaces to urban evaporation. *Water Resour. Res.* **50**: 2889–2902. https://doi.org/10.1002/2013WR013909.

Shepherd JM. 2005. A review of current investigations of urban-induced rainfall and recommendations for the future. *Earth Interact.* **9**: 1–27. https://doi.org/10.1175/EI156.1.

Shuttleworth WJ. 1978. A simplified one-dimensional theoretical description of the vegetation-atmosphere interaction. *Bound.-Layer Meteorol.* **14**: 3–27. https://doi.org/10.1007/BF00123986.

Sivakumar B, Sharma A. 2008. A cascade approach to continuous rainfall data generation at point locations. *Stoch. Environ. Res. Risk Assess.* **22**: 451–459. https://doi.org/10.1007/s00477-007-0145-y.

Spronken-Smith RA, Oke TR, Lowry WP. 2000. Advection and the surface energy balance across an irrigated urban park. *Int. J. Climatol.* **20**: 1033–1047.

Srikanthan R, McMahon TA. 2001. Stochastic generation of annual, monthly and daily climate data: a review. *Hydrol. Earth Syst. Sci.* **5**: 653–670. https://doi.org/10.5194/hess-5-653-2001.

Stewart ID, Oke TR. 2012. Local climate zones for urban temperature studies. *Bull. Am. Meteorol. Soc.* **93**: 1879–1900. https://doi.org/10.1175/BAMS-D-11-00019.1.

Sun T, Wang ZH, Oechel W, Grimmond S. 2017. The analytical objective hysteresis model (AnOHM v1.0): methodology to determine bulk storage heat flux coefficients. *Geosci. Model Dev. Discuss.* **2017**: 1–25. https://doi.org/10.5194/gmd-2016-300.

Wang Y, He B, Takase K. 2009. Effects of temporal resolution on hydrological model parameters and its impact on prediction of river discharge/Effets de la résolution temporelle sur les paramètres d'un modèle hydrologique et impact sur la prévision de l'écoulement en rivière. *Hydrol. Sci. J.* **54**: 886–898.

Ward HC, Grimmond CSB. 2017. Assessing the impact of changes in surface cover, human behaviour and climate on energy partitioning across greater London. *Landsc. Urban Plan.* **165**: 142–161. https://doi.org/10.1016/j.landurbplan.2017.04.001.

Ward HC, Evans JG, Grimmond CSB. 2013. Multi-season eddy covariance observations of energy, water and carbon fluxes over a suburban area in Swindon, UK. *Atmos. Chem. Phys.* **13**: 4645–4666. https://doi.org/10.5194/acp-13-4645-2013.

Ward HC, Evans JG, Grimmond CSB. 2015. Infrared and millimetre-wave scintillometry in the suburban environment – part 2: large-area sensible and latent heat fluxes. *Atmos. Meas. Tech.* **8**: 1407–1424. https://doi.org/10.5194/amt-8-1407-2015.

Ward HC, Kotthaus S, Järvi L, Grimmond CSB. 2016. Surface urban energy and water balance scheme (SUEWS): development and evaluation at two UK sites. *Urban Clim.* **18**: 1–32. https://doi.org/10.1016/j.uclim.2016.05.001.

Ward HC, Järvi L, Onomura S, Lindberg F, Grimmond CSB. 2017. SUEWS manual: version 2017a, http://www.met.reading.ac.uk/micromet (accessed 10 February 2017).

Weedon GP, Gomes S, Viterbo P, Shuttleworth WJ, Blyth E, Österle H, Adam JC, Bellouin N, Boucher O, Best M. 2011. Creation of the WATCH forcing data and its use to assess global and regional reference crop evaporation over land during the twentieth Century. *J. Hydrometeorol.* **12**: 823–848. https://doi.org/10.1175/2011JHM1369.1.

Weedon GP, Balsamo G, Bellouin N, Gomes S, Best MJ, Viterbo P. 2014. The WFDEI meteorological forcing data set: WATCH forcing data methodology applied to ERA-interim reanalysis data. *Water Resour. Res.* **50**: 7505–7514. https://doi.org/10.1002/2014WR015638.

Willems P, Vrac M. 2011. Statistical precipitation downscaling for small-scale hydrological impact investigations of climate change. *J. Hydrol.* **402**: 193–205. https://doi.org/10.1016/j.jhydrol.2011.02.030.

Wouters H, Demuzere M, Ridder KD, van Lipzig NPM. 2015. The impact of impervious water-storage parametrization on urban climate modelling. *Urban Clim.* **11**: 24–50. https://doi.org/10.1016/j.uclim.2014.11.005.

Xiao Q, McPherson EG, Simpson JR, Ustin SL. 2007. Hydrologic processes at the urban residential scale. *Hydrol. Processes* **21**: 2174–2188. https://doi.org/10.1002/hyp.6482.

Zhong S, Yang X-Q. 2015. Mechanism of urbanization impact on a summer cold-frontal rainfall process in the greater Beijing metropolitan area. *J. Appl. Meteorol. Climatol.* **54**: 1234–1247. https://doi.org/10.1175/JAMC-D-14-0264.1.